The Journal of Veterinary Medical Science

FULL PAPER

Pathology

Properties of macrophages and lymphocytes appearing in rat renal fibrosis followed by repeated injection of cisplatin

Satoshi MATSUYAMA[1)#], Munmun PERVIN[1,2)#], Minto NAKAGAWA[1)], Takeshi IZAWA[1)], Mitsuru KUWAMURA[1)] and Jyoji YAMATE[1)*]

[1)]Laboratory of Veterinary Pathology, Graduate School of Life and Environmental Sciences, Osaka Prefecture University, 1-58 Rinku-Ourai-Kita, Izumisano-shi, Osaka 598-8531, Japan

[2)]Department of Pathology, Faculty of Veterinary Science, Bangladesh Agricultural University, Mymensingh-2202, Bangladesh

ABSTRACT. Properties of macrophages and lymphocytes appearing in renal fibrosis remains to be investigated. F344 rats were injected once a week with cisplatin (2 mg/kg body weight) for 8 weeks and examined at post-final injection weeks 1, 3, 6, 9, and 12. Rats developed progressive renal fibrosis at weeks 1 to 6 as fibrosis-progress phase, and subsequent amelioration at weeks 9 and 12. CD68$^+$ M1-macrophages and major histocompatibility complex (MHC) class II$^+$ macrophages remarkably increased persistently, whereas CD163$^+$ M2-macrophages slightly increased. MHC class II$^+$/CD68$^+$ and MHC class II$^+$/CD163$^+$ macrophages were present, indicating that MHC class II$^+$ macrophages might have both functions of M1- and M2-macrophages. In the fibrosis-progress phase, interleukin (IL)-6, tumor necrosis factor (TNF)-α, and interferon (IFN)-γ for M1-factors, and transforming growth factor (TGF)-β1 and IL-10 for M2-factors tended to increase; tissue injury by M1 and fibrosis by M2 might have occurred simultaneously. Lots of CD4$^+$ and CD8$^+$ T cells appeared in close relation with MHC class II$^+$ macrophages, and mainly CD4$^+$ T cells formed aggregations. In the lymphocyte aggregates collected by laser microdissection, expression of IL-17A (for Th17 cells) and forkhead box P3 (FoxP3) (for Treg) significantly increased at weeks 1 and 6, respectively; presumably, Th17 cells might be involved in tissue injury, whereas Treg might be related to fibrosis amelioration. These results suggested that macrophages and T cells may contribute interrelatedly to renal fibrosis.

KEY WORDS: cisplatin, macrophage, T cell, rat, renal fibrosis

J. Vet. Med. Sci.
83(9): 1435–1442, 2021
doi: 10.1292/jvms.21-0341

Received: 11 June 2021
Accepted: 12 July 2021
Advanced Epub:
22 July 2021

Regardless of initial causes, renal fibrosis is the common final pathway in chronic kidney disease (CKD) [4, 34]. The fibrosis leads occasionally to renal dysfunction, and the patients with CKD need therapies to improve renal function (such as dialytic treatment) or transplantation [4]. Renal fibrosis is considered to be the risk factor of cardiovascular disease such as arteriosclerosis and brain stroke [19]. Therefore, the pathogenesis of renal fibrosis should be clarified, in order to prevent and improve CKD. Cisplatin (CDDP) is an anti-cancer drug that has nephrotoxicity as a side effect. CDDP damages the epithelium of proximal renal tubules, especially in the S_3 segment, and thereafter, induces renal interstitial fibrosis at the advanced stages [14, 31]. In renal injury in rats injected by a single injection of CDDP (6 mg/kg body weight (BW)), it is reported that macrophages with heterogeneous immunophenotypes, and lymphocytes, mainly T cells, participated in the pathology of renal fibrosis [14]. In the present study, we induced greater renal damage in rats by repeated injections of CDDP (2 mg/kg BW, once a week for 8 weeks), and analyzed the properties of macrophages and lymphocytes appearing after the cessation of the injection. In particular, we focused on major histocompatibility complex (MHC) class II-expressing macrophages, which may stimulate lymphocyte infiltration and regulates the fibrosis conditions [8, 12, 14, 35] and MHC class II macrophages are known to play important role in normal tissue genesis as the modeling (vs. remodeling of fibrosis) [11, 36].

*Correspondence to: Yamate, J.: yamate@vet.osakafu-u.ac.jp
#These authors contributed equally to this work.

MATERIALS AND METHODS

Animals and experimental procedures

A total of twenty-four male F344/DuCrj rats (5 weeks old; 106–146 g; Charles River Japan, Hino, Japan) were housed in an animal room controlled at 22 ± 2°C and with a 12 hr light-dark cycle and fed a standard diet (DC-8, CLEA, Tokyo, Japan) and tap water *ad libitum*. After one-week of acclimatization, twenty rats were injected with CDDP intraperitoneally once a week for 8 weeks at a dose of 2 mg/kg BW. At the post-final injection (PFI) weeks 1, 3, 6, 9 and 12, four rats were examined each. Four rats as controls received an equal volume of phosphate buffer saline (PBS) in the same manner and were examined at PFI week 1. All rats were euthanized under deep isoflurane anesthesia.

Experimental procedures were in agreement with institutional guidelines (approved by the ethical committee of Osaka Prefecture University; Nos. 23-24 and 25-85) for the Care and Use of Experimental Animals and were conducted in accordance with basic policies for the conduct of animal experimentation of the Ministry of Health, Labor and Welfare Standards relating to the Care and Management of Experimental Animals and the Act on Welfare and Management of Animals, Japan.

Histopathology and immunohistochemistry

Kidneys were immediately fixed in a 10% neutral buffered formalin or periodate-lysine-paraformaldehyde (PLP) solution. Deparaffinized sections were stained with hematoxylin and eosin (HE) for morphological observations. PLP-fixed deparaffinized tissue sections were immunostained with mouse monoclonal antibodies specific for CD68 (clone ED1, IgG1, 1:500, AbD Serotec, Oxford, UK), CD163 (clone ED2, IgG1, 1:300, AbD Serotec), MHC class II (clone OX6, IgG1, 1:1,000, AbD Serotec), CD4 (clone W3/25, IgG1, 1:2,000, AbD Serotec), CD8 (clone OX-8, IgG1, 1:200, AbD Serotec) and CD79α (clone HM57, IgG1κ, 1:5, Nichirei Bioscience Inc. Tokyo, Japan) using Histostainer (Nichirei Bioscience Inc.). Briefly, sections were incubated with 5% skimmed milk for 10 min, followed by 1 hr incubation with the primary antibody. After treatment with 3% H_2O_2 for 15 min, horseradish peroxidase-conjugated secondary antibody (Histofine Simple Stain MAX PO®; Nichirei Bioscience Inc.) was applied for 30 min. Positive reactions were visualized with 3, 3′-diaminobezidine tetrahydrochloride (DAB substrate kit, Nichirei Bioscience Inc.), and the sections were lightly counterstained with hematoxylin. For negative controls, tissue sections were treated with non-immunized mouse serum instead of the primary antibody.

Reverse-transcription polymerase chain reaction (RT-PCR) and laser microdissection (LMD)

Renal samples were collected from the affected cortico-medullary junction (corresponding roughly to the outer segment of the outer medulla) and immediately immersed in RNAlater reagent (Qiagen, Hilden, Germany). Total RNA was extracted with an SV total RNA isolation system (Promega, Fitchburg, WI, USA) and was reverse transcribed to cDNA with SuperScript VILO reverse transcriptase (Life technologies, Carlsbad, CA, USA). Real-time PCR was performed with SYBR Green Real-time PCR Master Mix (Toyobo Co., Ltd., Osaka, Japan) in a PicoReal 96 Real-time PCR system (Thermo Scientific, Waltham, MA, USA). Primers used were as follows: interleukin (IL)-6 (forward, tccgtttctacctggagtttgtg; reverse, agagcattggaagttggggtag), interferon (IFN)-γ (forward, tcgcacctgatcactaacttcttc; reverse, cgactccttttccgcttcc), tumor necrosis factor (TNF)-α (forward, tgcctcagcctcttctcattc; reverse, gctcctctgcttggtggttt), IL-1β (forward, gcaccttcttttccttcatctttg; reverse, tttgtcgttgcttgtctctcctt), transforming growth factor (TGF)-β1 (forward, cttcagctccacagagaagaactgc; reverse, cacgatcatgttggacaactgctcc), IL-10 (forward, ctgtcatcgatttctcccctgt; reverse, cagtagatgccgggtggttc), FoxP3 (forward, cttgtttgctgtgcggagac; reverse, tgagggtggcataggtgaaa) and β-actin (forward, taagaccctctatgccaacac; reverse, ctcctgcttgctgatccacat). For analysis of IL-17A expression, real-time PCR was performed with Thunderbird Probe qPCR Mix (Toyobo Co., Ltd.) with TaqMan Gene Expression Assays (Rn01757168_m1, Life Technologies). The data were analyzed using the comparative Ct method ($^{\Delta\Delta}C_t$ method) and were normalized to β-actin mRNA as an internal control. For LMD, 10-micrometer fresh frozen sections of the controls and affected kidneys at PFI weeks 1, 6 and 12 were prepared on foil slides (Leica Microsystems, Wetzlar, Germany). Sections were fixed in 19:1 ethanol/acetic acid for 3 min and were stained with 0.01% toluidine blue. The cortico-medullary junction areas of controls and the affected kidneys with lymphocyte aggregation were confirmed under microscopic observation, and were isolated with the LMD7000 system (Leica Microsystems). The LMD-isolated samples were subjected to RNA extraction followed by RT-PCR for FoxP3, and IL-17A as mentioned above.

Double immunofluorescence

To investigate the co-localization between macrophage-specific antigens, double immunofluorescence was carried out using antibody against MHC class II in combination with CD68 or CD163 antibody in fresh-frozen renal tissue sections (10 μm thick) from the control and CDDP-injected rats. Briefly, after fixation in acetone: methanol (1:1) for 10 min at 4°C, the sections were incubated with 10% normal goat serum for 30 min. The sections reacted with the primary antibody overnight at 4°C. After rinsing with PBS, the sections were incubated for 45 min with the following secondary antibodies: Alexa568/anti-mouse IgG1, Alexa488/anti-mouse IgG2a (Invitrogen Co., ×1,000). The sections were visualized with Vectashield mounting medium containing 4', 6-diamidino-2-phenylindole (DAPI; Vector Laboratories Inc.) for nuclear staining and analyzed using a virtual slide scanner (VS-120, Olympus, Tokyo, Japan).

Statistics and evaluation of immunopositive cells

Difference between control and CDDP-injected rats were evaluated by Dunnet's test. Values of $P<0.05$ were considered significant. The immunopositive cells in the affected cortico-medullary junction were evaluated semi-quantitatively as follows: -,

no immunopositive cells; ±, a few immunopositive cells, sporadically; +, a small number of immunopositive cells, sporadically or diffusely; ++, a moderate number of immunopositive cells, diffusely or focally; and +++, a large number of immunopositive cells, diffusely, focally or aggregately (for lymphocytes) (Tables 1–3). In addition, a semiquantitative evaluation was made for interstitial fibrosis degree according to that of our previous study [14]: no-fibrosis (−), slight degree (1+), moderate degree (2+), severe degree (3+) and more severe degree (4+) in the affected cortico-medullary region.

RESULTS

Renal fibrosis followed by repeated injections of CDDP

Control rats showed no renal lesions (fibrosis degree; –) (Fig. 1A). In CDDP-injected rats at PFI weeks 1 (2+ or 3+), 3 (3+ or 4+), and 6 (3+ or 4+), epithelial cells of proximal renal tubules, especially in the cortico-medullary junction showed necrosis/desquamation or subsequent regeneration (Fig. 1B and 1C). Fibrotic lesions developed around the damaged renal tubules and gradually progressed, with the most prominent at PFI week 6 (Fig. 1C and 1D). Afterward, the fibrotic lesions were gradually ameliorated at PFI weeks 9 (2+) and 12 (1+ or 2+) by regeneration of some renal epithelial cells; however, the fibrotic lesions were

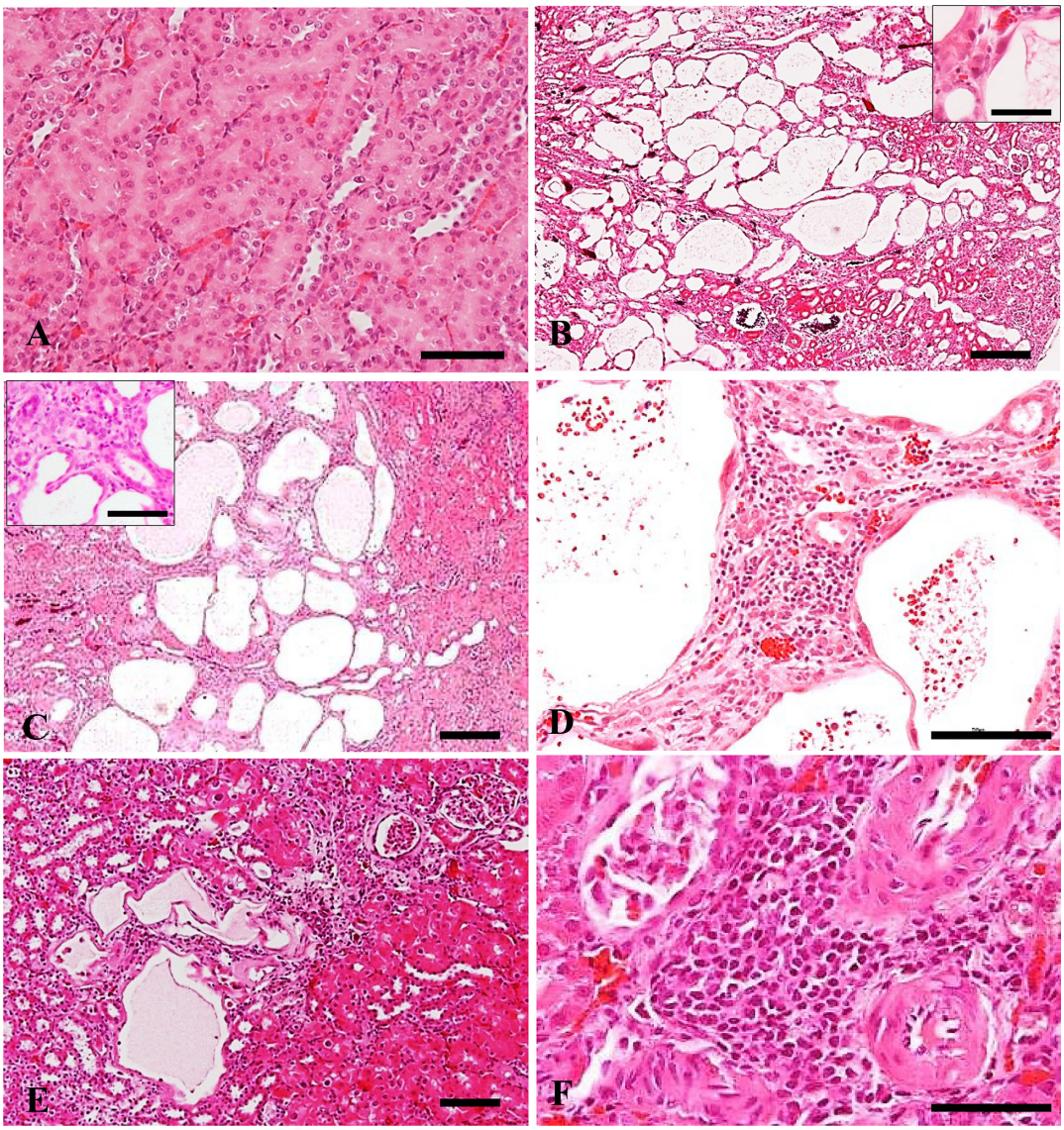

Fig. 1. Histopathological findings of control (A) and renal fibrosis lesions followed by repeated injection cisplatin (B–F). No histopathological change is observed in the kidneys of control rats **(A)**. At post-final injection (PFI) week 1 **(B)**, damaged renal tubules are variously dilated and atrophied; regenerating epithelia of these tubules are flattened (B, inset) or cuboidal in shape. At week 6 **(C)**, developing fibrotic lesions (C; inset at high magnification) and infiltrating lymphocytes **(D)** in the fibrotic area are observed diffusely around the cystic dilated tubules. At week 12, renal lesion is ameliorated **(E)** and infiltrating lymphocytes forms aggregation **(F)**. Hematoxylin and eosin stain, A, B, C, and E, bar=100 µm; inset of B, bar=30 µm; inset of C, bar=20 µm, D, bar=50 µm; F, bar=40 µm.

Table 1. Semi-quantitative evaluation of major histocompatibility complex (MHC) class II$^+$, CD68$^+$ and CD163$^+$ macrophages in rat renal fibrosis followed by repeated injection of cisplatin

PFI week	1	3	6	9	12	Control
MHC class II	++	+++	+++	++	++	-
CD68 (M1 macrophage)	+++	++	++	++	++	±
CD163 (M2 macrophage)	±	+	+	+	+	-

The evaluation methods were mentioned in Materials and Methods. PFI; post-final injection.

not completely resolved (Fig. 1E). There were no marked differences between rats at each point examined. In the present renal lesions, therefore, roughly, the fibrosis-progress phase was regarded at PFI weeks 1 to 6, whereas the fibrosis-amelioration phase at PFI weeks 9 and 12. Regenerating tubular epithelial cells were flattened or cuboidal in shape (Fig. 1B, inset) and the damaged renal tubules were irregularly diluted variously or atrophied at PFI weeks 1, 3, and 6 (Fig. 1B–D). The fibrotic lesions were thin around the markedly dilated renal tubules (Fig. 1C). In addition, around the damaged renal tubes, infiltration of macrophages and lymphocytes (as mentioned in detail below) began to be seen sporadically or diffusely as far as PFI week 1; afterward, the lymphocyte infiltration was increased diffusely or focally with time at PFI weeks 1, 6 and 12 (Fig. 1D and 1F), and occasionally formed aggregations around the damaged tubules at PFI weeks 6 and 12 (Fig. 1F).

Immunohistochemistry for renal macrophages

The appearance of renal macrophages reacting to MHC class II, CD68, and CD163 is shown in Table 1. MHC class II$^+$ macrophages were seen at a high level throughout the observation period (Table 1), with the greatest at PFI weeks 3 and 6 (Fig. 2A). MHC class II$^+$ macrophages were seen especially around the damaged renal tubes, being accompanied by lymphocytes. CD68$^+$ macrophages were frequently observed as early as PFI week 1, and they remained increased levels at PFI weeks 3 to 12 (Table 1). The distribution of CD68$^+$ macrophages corresponded almost to that of MHC II$^+$ macrophages; that is, their infiltration was diffusely or focally seen around the damaged tubules (Fig. 2B). As compared with the appearance of MHC class II$^+$ and CD68$^+$ macrophages, CD163$^+$ macrophages were much less; CD163$^+$ macrophages were slightly increased at PFI weeks 3 to 12, and were sporadically distributed in the thin fibrotic lesions occurring around the dilated renal tubules at PFI weeks 3 and 6 (Fig. 2C and 2D, Table1). Such thin fibrotic lesions around the markedly dilated renal tubules have been reported characteristically in CDDP-treated rat renal fibrosis in our previous study [14], but the degree was more prominent in the present study.

M1/M2-polarization of MHC class II$^+$ macrophages

CD68$^+$ macrophages are regarded as M1 type (classically activated macrophages), whereas M2 macrophages (alternatively activated macrophages) work through CD163 expression [25, 26, 30]. MHC class II$^+$/CD68$^+$ macrophages increased at PFI weeks 1 to 6 (Fig. 2D–F), showing the peak at PFI week 6, and then, they gradually decreased at PFI weeks 9 and 12 (Table 2). Although the number was small, MHC class II$^+$/CD163$^+$ macrophages increased at PFI weeks 3 to 12 (Fig. 2G–I). At PFI weeks 1 to 6, MHC class II$^+$/CD68$^+$ macrophages were seen more predominantly than MHC class II$^+$/CD163$^+$ macrophages, but, at PFI weeks 9 and 12, the appearance level was similar between MHC class II$^+$/CD68$^+$ cells and MHC class II$^+$/CD163$^+$ macrophages (Table 2).

Immunohistochemistry for lymphocytes

CD4$^+$ T cells were consistently seen at the high level throughout the observation period, showing the greatest at PFI weeks 3, 6, and 9 (Table 3). CD8$^+$ T cells increased at PFI week 1, and afterward, become more severe at PFI weeks 3 to 12 (Table 3). CD4$^+$ T cells were seen focally or aggregately (Fig. 3A), whereas CD8$^+$ T cells tended to be diffusely distributed in the affected cortex-medullary junction, and some were included in the aggregation (Fig. 3B). On the other hand, the number of CD79α$^+$ B cells were much smaller during the observation period, in contrast to CD4$^+$ and CD8$^+$ T cells (Table 3), and they were sporadically distributed only around the affected renal tubules (Fig. 3C).

mRNA expressions of inflammatory factors

Renal expression of IL-6, IFN-γ, and TGF-β1 mRNA showed a significant increase at weeks 1 to 6 (except at PFI week 6 for IL-6) (figures not shown). TNF-α and IL-10 significantly increased at PFI week 6 and at PFI weeks 6 and 12, respectively. IL-4 and IL-1β did not show any significant change. To investigate the detailed properties of lymphocytes, IL-17A and FoxP3 mRNA expressions were analyzed using samples of controls and at PFI weeks 1, 6, and 12 obtained by LMD. Expression of IL-17A and FoxP3 showed a significant increase at PFI week 1 and at PFI week 6, respectively (Fig. 4).

DISCUSSION

Renal fibrosis followed by repeated injections of CDDP

A single injection of CDDP (6 mg/kg BW) induces epithelial degeneration, necrosis and desquamation in the proximal renal tubules in the cortico-medullary junction, and then, fibrotic lesion develops in the interstitium of the affected areas [14, 29, 33]. In the present study, CDDP at the low dose of 2 mg/kg BW was injected once a week for 8 weeks, and after the cessation of injection,

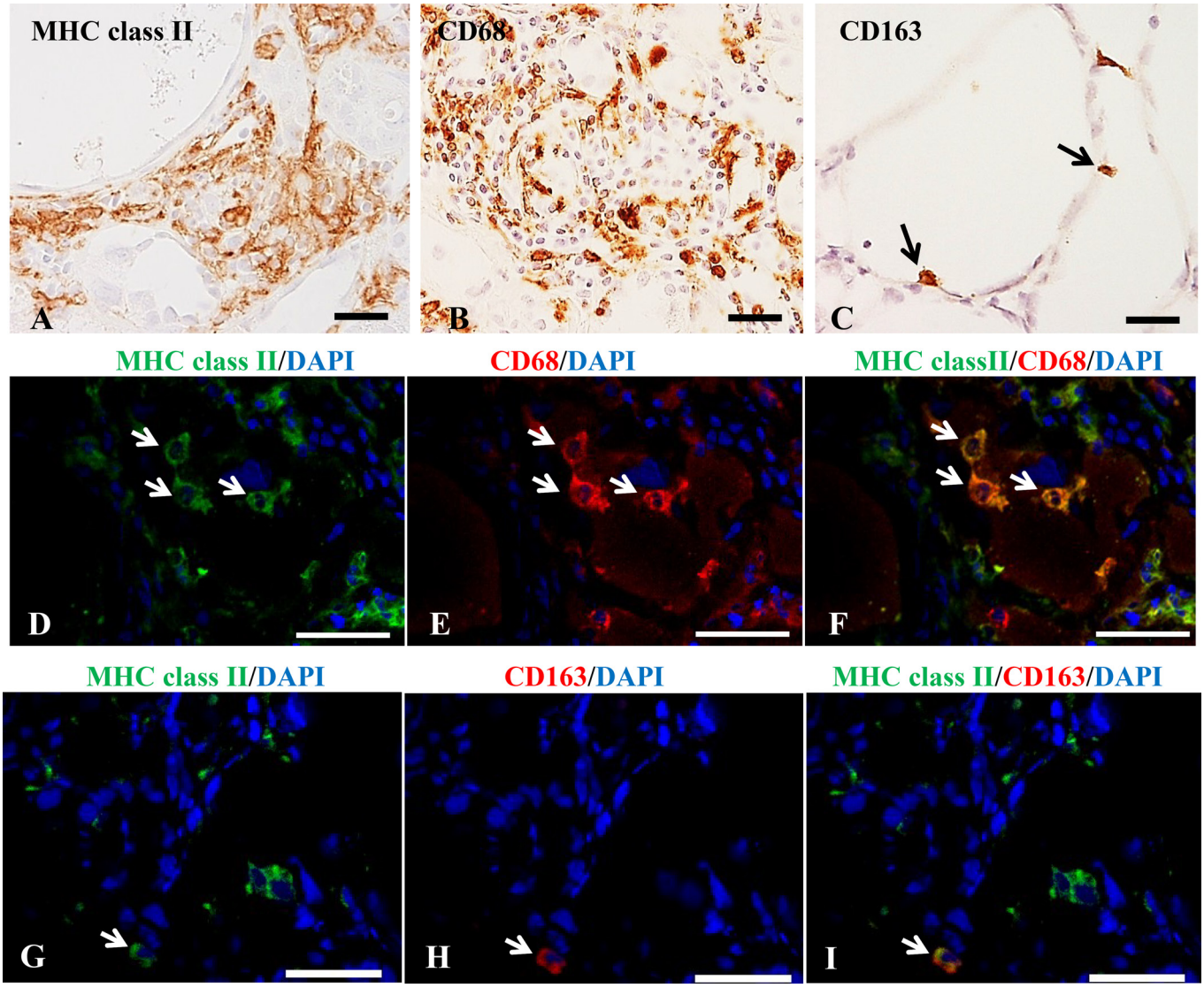

Fig. 2. Immunohistochemistry (A–C) and immunofluorescence (D–I) for macrophage markers at PFI week 6. Major histocompatibility complex (MHC) class II$^+$ macrophages are focally observed around the damaged renal tubules **(A)**. CD68$^+$ M1 macrophages are distributed in fibrotic region **(B)**, whereas CD163$^+$ M2 macrophages are sporadically seen in thin fibrotic lesion around the markedly dilated renal tubules (arrows) **(C)**. MHC class II$^+$/CD68$^+$ M1 macrophages **(D–F)** and MHC class II$^+$/CD163$^+$ M2 macrophages **(G–I)** are present. Arrows indicate the representative double positive cells. 4', 6-diamidino-2-phenylindole (DAPI) for nuclear stain. Bar=50 µm.

Table 2. Semi-quantitative analyses of MHC class II$^+$/CD68$^+$ M1- and MHC class II$^+$/CD163$^+$ M2-macrophages in rat renal fibrosis followed by repeated injection of cisplatin

PFI week	1	3	6	9	12
MHC class II/CD68	±	+	++	+	±
MHC class II/CD163	-	±	+	+	±

The evaluation methods were mentioned in Materials and Methods. PFI; post-final injection.

Table 3. Semi-quantitative evaluation of CD4$^+$, CD8$^+$ and CD79α$^+$ lymphocytes in rat renal fibrosis followed by repeated injection of cisplatin

PFI week	1	3	6	9	12	Control
CD4 T cell	++	+++	+++	+++	++	-
CD8 T cell	+	++	++	++	++	-
CD79α B cell	-	±	+	±	±	-

The evaluation methods are mentioned in Materials and Methods. PFI; post-final injection.

the gradually affected kidneys developed interstitial fibrosis at PFI weeks 1 to 6 with the maximum at week 6 as the fibrosis-progress phase, and then, recovered to some degree (incompletely) at PFI weeks 9 and 12 as the fibrosis-amelioration phase. The appearance of α-smooth muscle actin-positive myofibroblasts capable of producing collagens has been reported in fibrotic lesions [32]. These histopathological findings were in agreement with those reported previously [32]. Throughout the observation period, along with macrophages, lymphocyte reaction was characteristically seen, sometimes forming aggregations as follicles around the damaged

renal tubules. Lymphocyte appearance was much greater in the present low-dose experiment, indicating better samples to analyze the properties of lymphocytes.

M1/M2 macrophage polarization

In rat renal fibrosis induced by a single injection of CDDP of which experiment was observed until 20 days after the injection, $CD68^+$ M1 macrophages began to increase after injury of renal tubules and subsequently, $CD163^+$ M2 macrophages showed a gradual increase with fibrosis; there was M1/M2-polarization [14]. In the present study, during the observation period at PFI weeks 1 to 12, $CD68^+$ M1 macrophages showed a consistent, remarkable increase, and $CD163^+$ M2 macrophages were also increased, although the appearance of $CD163^+$ M2 macrophages was much less than $CD68^+$ M1 macrophages (Table 1). Generally, M1 macrophages induce tissue injury and inflammation by producing factors such as IL-6, TNF-α and IFN-γ, whereas M2 macrophages contribute to the resolution of inflammation and the promotion of tissue fibrosis through produced TGF-β1, IL-1β and IL-10 [9, 21, 30]. In the present study, IL-6, TNF-α and IFN-γ for M1-factors, as well as TGF-β1 and IL-10 for M2-factors tended to increase mainly at PFI weeks 1, 3 or 6. In the fibrosis-progress phase, that is, tissue injury by M1 macrophages and fibrosis by M2 macrophages might have occurred simultaneously. It is also reported that M1- and M2-macrophages contributed simultaneously to the development of hepatic pseudolobules (chronic lesions) in rat cirrhosis induced by repeated injection of thioacetamide, a hepatotoxicant [24]. In the fibrosis-amelioration phase at weeks 9 and 12, there were still many $CD68^+$ M1 macrophages. CD68 is a member of the lysosomal/endosomal-associated membrane glycoprotein family, which may play roles in phagocytosis [15]. $CD68^+$ M1 macrophages seen at PFI weeks 9 and 12 might have contributed to the removal of cell debris for the amelioration of fibrosis (reparative fibrosis).

MHC class II^+ macrophages and lymphocytes

Macrophages reacting to MHC class II were increased consistently during the observation period; the cells appeared to be the greatest among macrophage populations (Table 1). MHC class II^+ macrophages were also seen in renal fibrosis induced by a single injection of CDDP [14]. However, their functional properties remain to be investigated. In double immunofluorescence, there were MHC class $II^+/CD68^+$ M1 macrophages and MHC class $II^+/CD163^+$ M2 macrophages (Table 2), indicating that MHC class II^+ macrophages might have both inflammatory and anti-

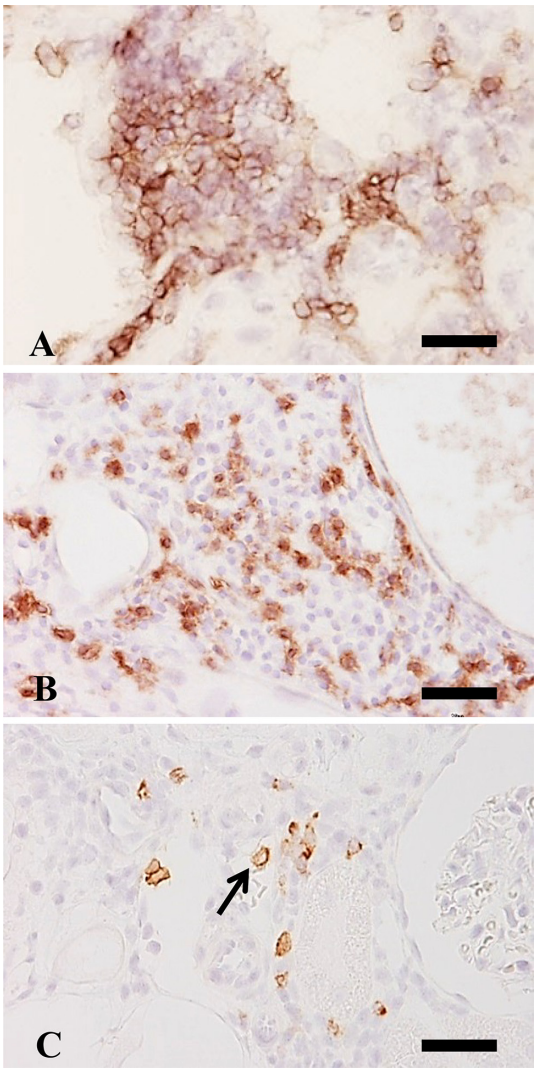

Fig. 3. Immunohistochemistry for lymphocyte markers at PFI week 6. Many $CD4^+$ T cells are seen in fibrotic region, forming aggregation like follicle **(A)**. $CD8^+$ T cells are diffusely seen in the affected area **(B)**. A few $CD79\alpha^+$ B cells are sporadically present (arrows) **(C)**. Counterstained with hematoxylin. Bar=20 µm.

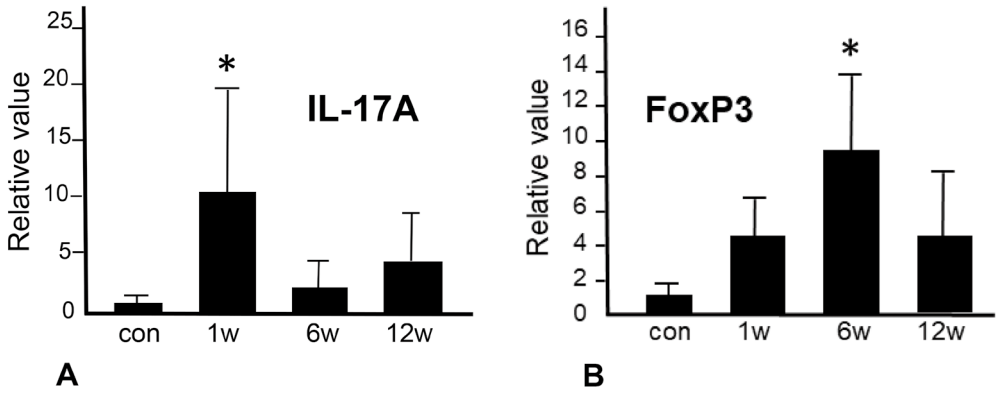

Fig. 4. mRNA expressions of interleukin (IL)-17α **(A)** and forkhead box P3 (FoxP3) **(B)** by the real-time PCR using samples of controls, and focal and aggregated lymphocytes at PFI weeks 1, 6 and 12. The expressions were normalized against β-actin mRNA as internal control gene. Dunnet's test, *, $P<0.05$, significantly different from the control.

inflammatory functions in renal fibrosis. Macrophages expressing MHC class II are regarded as M1 type in chemical-induced rat hepatic fibrosis [13, 22, 25, 26], whereas those are polarized toward M2 type in experimentally-induced rat myocardial fibrosis [2]. M1 and M2 macrophages could have expressed MHC class II under unknown microenvironmental conditions [3].

More interestingly, MHC class II$^+$ macrophages were localized mainly around damaged renal tubes throughout the observation period, apparently in close relation with infiltrating lymphocytes. It is reported that MHC class II expression is related to the subsequent induction of CD4$^+$ T cells through the complicated immune system [20]. Because CD4$^+$ T cells stimulate macrophages to generate inflammatory mediators [18], and MHC class II$^+$ macrophages are known to present the processed antigens to CD4$^+$ T cells [1, 7], CD4$^+$ T cells may act with the relation of MHC class II$^+$ macrophages. In fact, it is likely that CD4$^+$ T cells contribute to the progress of renal fibrosis [1, 28]. In the present study, additionally, CD8$^+$ T cells also showed an increased number at PFI weeks 3–12, although the appearance of CD8$^+$ T cells was less than CD4$^+$ T cells. In renal fibrosis induced by a single injection, CD4$^+$ and CD8$^+$ T cells are also seen in the fibrotic lesions [14]; CD8$^+$ T cells may be able to mediate cytotoxicity to tubular cells [23].

Detailed functions of focal or aggregated lymphocytes were analyzed using samples obtained by LMD method at PFI weeks 1, 6 and 12. IL-17A was significantly increased at PFI week 1, and by RT-PCR, increased levels of IL-6 and TGF-β1 were also confirmed in the fibrosis progression phase as mentioned above. Generally, naïve T cells differentiate to Th17 cells under influence of IL-6 or TGF-β1 [17]. Th17 cells, which may be mainly involved in inflammation of autoimmune diseases [17], are a subtype of CD4$^+$ T cells. The focal or aggregated lymphocytes might be capable of producing IL-17A, which could stimulate inflammation via cytokines such as TNF-α [16, 27]. At PFI week 6, FoxP3 expression significantly increased in focal or aggregated lymphocytes. FoxP3 is a transcriptional factor and used as a regulatory T cell (Treg) marker. It is considered that Treg could attenuate fibrosis in tissue remodeling after injury [5, 6]. The increased FoxP3 might have been related to the induction of fibrosis-amelioration phase at PFI weeks 9 to 12. The timing of increased FoxP3 expression at PFI week 6 in the present study might be a turning point between the fibrosis-progress and fibrosis-amelioration phases, although a more detailed analysis is needed.

Although CD79α$^+$ B cells were much less in appearance than CD4$^+$ and CD8$^+$ cells, B cells were present during the observation period, peaking at PFI week 6. A study on mouse unilateral ureteral obstruction model showed that the early-stage accumulation of B cells in the affected kidney might accelerate monocyte/macrophage infiltration, thereby leading to aggravated fibrosis [1]. The significance of B cells seen in this renal fibrosis remains to be investigated [14].

In conclusion, rat kidneys damaged by the repeated injection of CDDP developed progressive interstitial renal fibrosis at PFI weeks 1, 3 and 6, and subsequent amelioration at PFI weeks 9 and 12. CD68$^+$ M1 macrophages showed a consistent increase, and CD163$^+$ M2 macrophages were also increased but slightly. IL-6, TNF-α and IFN-γ for M1-factors, as well as TGF-β1 and IL-10 for M2-factors tended to increase mainly at PFI weeks 1, 3 or 6. Tissue injury by M1 macrophages and fibrosis by M2 macrophages might have occurred simultaneously, resulting in renal fibrosis in the fibrosis-progress phase. More interestingly, MHC class II$^+$ macrophages had functions of both M1 and M2 types in double immunofluorescence analyses, and apparently, they increased consistently in relation with increased numbers of T cells; these T cells, particularly CD4$^+$ T cells, might act with MHC class II$^+$ macrophages. The focal or aggregated lymphocytes obtained by LMD showed increased IL-17A (for Th17 cells) and FoxP3 (a marker of Treg); presumably, Th17 cells, a subtype of CD4$^+$ T cells, might be involved in tissue injury, whereas Treg might contribute to fibrosis amelioration. It is likely that M1/M2 macrophages and T cells reacting to CD4 and CD8 contribute complicatedly to renal fibrosis [8, 10]. This study is the first trial to analyze the properties of infiltrating cells in rat renal fibrosis followed by repeated injection of CDDP. The information would be useful for the understanding of the pathogenesis of CKD in dogs and cats; in particular, CKD is prevalent in elderly cats [12].

POTENTIAL CONFLICTS OF INTEREST. The authors have nothing to disclose.

ACKNOWLEDGMENTS. This work was supported partly by the JSPS KAKENHI Grant Number19H03130 (to Yamate); the Platform Project for Supporting Drug Discovery and Life Science Research (Basis for Supporting Innovative Drug Discovery and Life Science Research (BINDS)) from AMED under Grant Number JP21am0101123 (to Yamate).

REFERENCES

1. Han, H., Zhu, J., Wang, Y., Zhu, Z., Chen, Y., Lu, L., Jin, W., Yan, X. and Zhang, R. 2017. Renal recruitment of B lymphocytes exacerbates tubulointerstitial fibrosis by promoting monocyte mobilization and infiltration after unilateral ureteral obstruction. *J. Pathol.* **241**: 80–90. [Medline] [CrossRef]
2. Koga, M., Karim, M. R., Kuramochi, M., Izawa, T., Kuwamura, M. and Yamate, J. 2021. Appearance of heterogeneous macrophages during development of isoproterenol-induced rat myocardial fibrosis. *Toxicol. Pathol.* **49**: 1048–1061 [CrossRef]. [Medline]
3. Lech, M. and Anders, H. J. 2013. Macrophages and fibrosis: How resident and infiltrating mononuclear phagocytes orchestrate all phases of tissue injury and repair. *Biochim. Biophys. Acta* **1832**: 989–997. [Medline] [CrossRef]
4. Leung, K. C., Tonelli, M. and James, M. T. 2013. Chronic kidney disease following acute kidney injury-risk and outcomes. *Nat. Rev. Nephrol.* **9**: 77–85. [Medline] [CrossRef]
5. Li, J., Qiu, S. J., She, W. M., Wang, F. P., Gao, H., Li, L., Tu, C. T., Wang, J. Y., Shen, X. Z. and Jiang, W. 2012. Significance of the balance between regulatory T (Treg) and T helper 17 (Th17) cells during hepatitis B virus related liver fibrosis. *PLoS One* **7**: e39307. [Medline] [CrossRef]
6. Lim, A. I., Tang, S. C., Lai, K. N. and Leung, J. C. 2013. Kidney injury molecule-1: more than just an injury marker of tubular epithelial cells? *J. Cell. Physiol.* **228**: 917–924. [Medline] [CrossRef]
7. Liu, L., Kou, P., Zeng, Q., Pei, G., Li, Y., Liang, H., Xu, G. and Chen, S. 2012. CD4+ T Lymphocytes, especially Th2 cells, contribute to the

progress of renal fibrosis. *Am. J. Nephrol.* **36**: 386–396. [Medline] [CrossRef]
8. Luzina, I. G., Todd, N. W., Iacono, A. T. and Atamas, S. P. 2008. Roles of T lymphocytes in pulmonary fibrosis. *J. Leukoc. Biol.* **83**: 237–244. [Medline] [CrossRef]
9. Martinez, F. O. and Gordon, S. 2014. The M1 and M2 paradigm of macrophage activation: time for reassessment. *F1000Prime Rep.* **6**: 13. [Medline] [CrossRef]
10. Martín-Fernández, B., Rubio-Navarro, A., Cortegano, I., Ballesteros, S., Alía, M., Cannata-Ortiz, P., Olivares-Álvaro, E., Egido, J., de Andrés, B., Gaspar, M. L., de Las Heras, N., Lahera, V. and Moreno, J. A. 2016. Aldosterone induces renal fibrosis and inflammatory M1-macrophage subtype via mineralocorticoid receptor in rats. *PLoS One* **11**: e0145946. [Medline] [CrossRef]
11. Matsuyama, S., Karim, M. R., Izawa, T., Kuwamura, M. and Yamate, J. 2018. Immunohistochemical analyses of the kinetics and distribution of macrophages in the developing rat kidney. *J. Toxicol. Pathol.* **31**: 207–212. [Medline] [CrossRef]
12. McLeland, S. M., Cianciolo, R. E., Duncan, C. G. and Quimby, J. M. 2015. A comparison of biochemical and histopathologic staging in cats with chronic kidney disease. *Vet. Pathol.* **52**: 524–534. [Medline] [CrossRef]
13. Mosser, D. M. and Edwards, J. P. 2008. Exploring the full spectrum of macrophage activation. *Nat. Rev. Immunol.* **8**: 958–969. [Medline] [CrossRef]
14. Nakagawa, M., Karim, M. R., Izawa, T., Kuwamura, M. and Yamate, J. 2021. Immunophenotypical characterization of M1/M2 macrophages and lymphocytes in cisplatin-induced rat progressive renal fibrosis. *Cells* **10**: 257. [Medline] [CrossRef]
15. Nelson, M. P., Christmann, B. S., Dunaway, C. W., Morris, A. and Steele, C. 2012. Experimental Pneumocystis lung infection promotes M2a alveolar macrophage-derived MMP12 production. *Am. J. Physiol. Lung Cell. Mol. Physiol.* **303**: L469–L475. [Medline] [CrossRef]
16. Nestle, F. O., Kaplan, D. H. and Barker, J. 2009. Psoriasis. *N. Engl. J. Med.* **361**: 496–509. [Medline] [CrossRef]
17. Ogura, H., Murakami, M., Okuyama, Y., Tsuruoka, M., Kitabayashi, C., Kanamoto, M., Nishihara, M., Iwakura, Y. and Hirano, T. 2008. Interleukin-17 promotes autoimmunity by triggering a positive-feedback loop via interleukin-6 induction. *Immunity* **29**: 628–636. [Medline] [CrossRef]
18. Ricardo, S. D., van Goor, H. and Eddy, A. A. 2008. Macrophage diversity in renal injury and repair. *J. Clin. Invest.* **118**: 3522–3530. [Medline] [CrossRef]
19. Schiffrin, E. L., Lipman, M. L. and Mann, J. F. 2007. Chronic kidney disease: effects on the cardiovascular system. *Circulation* **116**: 85–97. [Medline] [CrossRef]
20. Schmid, A. B., Coppieters, M. W., Ruitenberg, M. J. and McLachlan, E. M. 2013. Local and remote immune-mediated inflammation after mild peripheral nerve compression in rats. *J. Neuropathol. Exp. Neurol.* **72**: 662–680. [Medline] [CrossRef]
21. Sica, A. and Mantovani, A. 2012. Macrophage plasticity and polarization: in vivo veritas. *J. Clin. Invest.* **122**: 787–795. [Medline] [CrossRef]
22. Tsuji, Y., Kuramochi, M., Golbar, H. M., Izawa, T., Kuwamura, M. and Yamate, J. 2020. Acetaminophen-induced rat hepatotoxicity based on M1/M2-macrophage polarization, in possible relation to damage-associated molecular patterns and autophagy. *Int. J. Mol. Sci.* **21**: 8998. [Medline] [CrossRef]
23. Wang, Y. and Harris, D. C. 2011. Macrophages in renal disease. *J. Am. Soc. Nephrol.* **22**: 21–27. [Medline] [CrossRef]
24. Wijesundera, K. K., Izawa, T., Murakami, H., Tennakoon, A. H., Golbar, H. M., Kato-Ichikawa, C., Tanaka, M., Kuwamura, M. and Yamate, J. 2014. M1- and M2-macrophage polarization in thioacetamide (TAA)-induced rat liver lesions; a possible analysis for hepato-pathology. *Histol. Histopathol.* **29**: 497–511. [Medline]
25. Wijesundera, K. K., Izawa, T., Tennakoon, A. H., Golbar, H. M., Tanaka, M., Kuwamura, M. and Yamate, J. 2015. M1-/M2-macrophages contribute to the development of GST-P-positive preneoplastic lesions in chemically-induced rat cirrhosis. *Exp. Toxicol. Pathol.* **67**: 467–475. [Medline] [CrossRef]
26. Wijesundera, K. K., Izawa, T., Tennakoon, A. H., Murakami, H., Golbar, H. M., Katou-Ichikawa, C., Tanaka, M., Kuwamura, M. and Yamate, J. 2014*a*. M1- and M2-macrophage polarization in rat liver cirrhosis induced by thioacetamide (TAA), focusing on Iba1 and galectin-3. *Exp. Mol. Pathol.* **96**: 382–392. [Medline] [CrossRef]
27. Witowski, J., Książek, K. and Jörres, A. 2004. Interleukin-17: a mediator of inflammatory responses. *Cell. Mol. Life Sci.* **61**: 567–579. [Medline] [CrossRef]
28. Wynn, T. A. 2008. Cellular and molecular mechanisms of fibrosis. *J. Pathol.* **214**: 199–210. [Medline] [CrossRef]
29. Yamamoto, E., Izawa, T., Juniantito, V., Kuwamura, M. and Yamate, J. 2010. Relationship of cell proliferating marker expressions with PGE_2 receptors in regenerating rat renal tubules after cisplatin injection. *J. Toxicol. Pathol.* **23**: 271–275. [Medline] [CrossRef]
30. Yamate, J., Izawa, T. and Kuwamura, M. 2016. Histopathological analysis of rat hepatotoxicity based on macrophage functions: in particular, an analysis for thioacetamide-induced hepatic lesions. *Food Saf (Tokyo)* **4**: 61–73. [Medline] [CrossRef]
31. Yamate, J., Machida, Y., Ide, M., Kuwamura, M., Kotani, T., Sawamoto, O. and LaMarre, J. 2005. Cisplatin-induced renal interstitial fibrosis in neonatal rats, developing as solitary nephron unit lesions. *Toxicol. Pathol.* **33**: 207–217. [Medline] [CrossRef]
32. Yamate, J., Sato, K., Ide, M., Nakanishi, M., Kuwamura, M., Sakuma, S. and Nakatsuji, S. 2002. Participation of different macrophage populations and myofibroblastic cells in chronically developed renal interstitial fibrosis after cisplatin-induced renal injury in rats. *Vet. Pathol.* **39**: 322–333. [Medline] [CrossRef]
33. Yamate, J., Sato, K., Machida, Y., Ide, M., Sato, S., Nakatsuji, S., Kuwamura, M., Kotani, T. and Sakuma, S. 2000. Cisplatin-induced rat renal interstitial fibrosis; a possible pathogenesis based on the data. *J. Toxicol. Pathol.* **4**: 237–247. [CrossRef]
34. Yamate, J., Okado, A., Kuwamura, M., Tsukamoto, Y., Ohashi, F., Kiso, Y., Nakatsuji, S., Kotani, T., Sakuma, S. and Lamarre, J. 1998. Immunohistochemical analysis of macrophages, myofibroblasts, and transforming growth factor-β localization during rat renal interstitial fibrosis following long-term unilateral ureteral obstruction. *Toxicol. Pathol.* **26**: 793–801. [Medline] [CrossRef]
35. Zhang, M. and Zhang, S. 2020. T Cells in Fibrosis and Fibrotic Diseases. *Front. Immunol.* **11**: 1142. [Medline] [CrossRef]
36. Zhang, M. Z., Yao, B., Yang, S., Jiang, L., Wang, S., Fan, X., Yin, H., Wong, K., Miyazawa, T., Chen, J., Chang, I., Singh, A. and Harris, R. C. 2012. CSF-1 signaling mediates recovery from acute kidney injury. *J. Clin. Invest.* **122**: 4519–4532. [Medline] [CrossRef]